

M.G. DA SILVA<sup>1</sup>  
H. VARGAS<sup>1</sup>  
A. MIKLÓS<sup>2</sup>  
P. HESS<sup>2,✉</sup>

## Photoacoustic detection of ozone using a quantum cascade laser

<sup>1</sup> Laboratório de Ciências Físicas – CCT, Universidade Estadual do Norte Fluminense, Av. Alberto Lamego, 2000 – Pq. Califórnia Campos dos Goytacazes – CEP: 28013-602 – RJ – Brazil<sup>TSa</sup>

<sup>2</sup> Institute of Physical Chemistry, University of Heidelberg, Im Neuenheimer Feld 253, 69120 Heidelberg, Germany

Received: 8 March 2004/Revised version: 16 March 2004

Published online: ■ ■ 2004 • © Springer-Verlag 2004

**ABSTRACT** A 9.5- $\mu\text{m}$  pulsed quantum cascade laser (QCL) and a differential photoacoustic (PA) detector were used to measure trace concentrations of  $\sim 100$  ppbv ozone at ambient pressure with high selectivity. The QCL was tuned by temperature variation between  $-41^\circ\text{C}$  and  $30.6^\circ\text{C}$  and the corresponding wavelengths were determined by the PA spectrum of  $\text{CO}_2$ . Good agreement was found between the measured PA spectrum and the simulated HITRAN spectrum of ozone. The PA signal showed a linear dependence on the ozone concentration in the investigated 4300–100 ppbv range. In comparison with recently published results, in which a similar QCL in combination with an optical absorption analysis technique was applied, an improvement in the ozone-detection sensitivity by a factor of about 200 was achieved.

**PACS** 42.62.Fi; 82.80.Kq; 82.80.Gk; 92.60.Sz

### 1 Introduction

The rapid development of quantum cascade lasers (QCLs) [1] has opened up new possibilities for real-time spectroscopic detection of various molecular species in the 3–5  $\mu\text{m}$  and 8–13  $\mu\text{m}$  atmospheric windows. Commercially available DFB (distributed feedback)-QCL devices are non-cryogenic, tunable, narrow-line-width light sources, which can be used in combination with different detection techniques. QCL-based absorption measurements of several trace gases have been published in recent years [2–9]. Most measurements were performed using sophisticated optical detection techniques; the alternative photoacoustic technique has been employed only in [2, 4].

In this publication, we present photoacoustic measurements of ozone with a DFB-QCL device. The research was motivated by the need for a simple, sensitive, and spectrally selective instrument for measuring trace concentrations

of ozone in urban air. While high sensitivity is ensured by UV photometry at 257 nm due to the very high absorption coefficient, the spectral selectivity is relatively low in this frequency range, because nearly all compounds containing oxygen absorb in the same range and the absorption bands are rather broad in the UV. An additional disadvantage of ozone detection with UV radiation is the photochemistry induced by the dissociation process, leading to highly reactive species and consequently to secondary reactions. In comparison, a lower sensitivity but much better spectral selectivity under reaction-free conditions can be achieved in the mid-IR, around 9.5  $\mu\text{m}$ .

About 85%–90% of atmospheric ozone is found in the stratosphere and plays an important role in protecting life against harmful UV radiation ('skin cancer'). Tropospheric or ground-level ozone, on the other hand, is the major ingredient in smog and continues to pose a health risk (it attacks cells and breaks down tissue, decreases the ability

to breathe, and increases the susceptibility to respiratory diseases). Ozone is also a plant toxin and is responsible for damage to agricultural crops and forests. As a strong oxidant and, together with water vapor, as a precursor of the hydroxyl radical (OH), ozone has a strong influence on the oxidizing power of the atmosphere and hence on the rate at which many natural and anthropogenic compounds are eliminated from the atmosphere. The amount in the troposphere over the continents in the northern hemisphere increased from about 10–20 ppbv in the late 19th century to the present-day background concentration of approximately 40–50 ppbv in urban areas [10]. However, in many cities inhabitants are periodically exposed to ozone concentrations that exceed the health-based air-quality standard of 120 ppbv.

A recent review of state-of-the-art ozone research from a molecular perspective, covering the photochemical, kinetic, and theoretical aspects of ozone isotope formation and reactions, can be found in [11].

### 2 Experimental setup

A simple experimental setup (Fig. 1), including a 9.5- $\mu\text{m}$  pulsed QCL as a versatile tunable light source and a differential photoacoustic (PA) detector [12], was employed to detect ozone at ambient pressure. The InGaAs–AlInAs/InP DFB-QCL source was a commercial single-frequency semiconductor laser (Alpes Lasers) designed for pulsed operation near room temperature. For the spectral experiment, the QCL was excited with 20-ns pulses at 400-kHz repetition rate (duty

✉ Fax: ■ ■ CE<sup>b</sup>, E-mail: peter.hess@urz.uni-heidelberg.de

<sup>TSa</sup> Please check address 1 (Brazil) for the correct style.  
<sup>CEb</sup> Please provide a fax number.

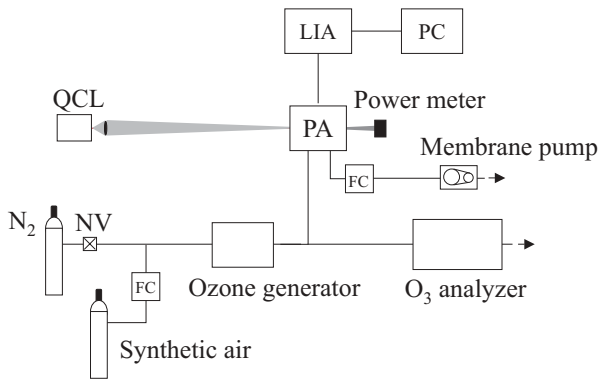


**FIGURE 1** Schematic of the experimental setup with gas supply and ozone analyzer. Abbreviations: QCL: quantum cascade laser with driver and temperature-controller electronics, LIA: lock-in amplifier, PC: personal computer, PA: photoacoustic detector with microphone preamplifier, NV: needle valve, FC: mass-flow controller

cycle 0.8%) and, for the determination of concentrations, a pulse duration of 50 ns was applied (duty cycle 2%). The QCL was modulated by an external TTL (transistor–transistor logic) signal at 3.8 kHz to excite the first longitudinal mode of the resonant differential PA cell (resonance enhancement  $Q = 36$ ). The photoacoustic signal was measured by a digital lock-in amplifier (Stanford SR850).

Ozone spectra were recorded in the spectral range of  $1046.3\text{--}1051.8\text{ cm}^{-1}$  by scanning the temperature of the QCL between  $-41\text{ }^{\circ}\text{C}$  and  $30.6\text{ }^{\circ}\text{C}$ . A germanium lens with an antireflection coating was applied to collimate the laser beam through the photoacoustic cell. Unfortunately, about 40% of the QCL power was lost because of the large divergence of the QCL beam. The transmitted light

power was measured by a pyroelectric sensor. The QCL power decreased with temperature from about 4.6 mW to about 2 mW during the temperature scan, operating at 2% duty cycle.

Gaseous ozone samples were produced by a commercial ozone generator based on an electrical discharge. Synthetic air (20.5%  $\text{O}_2$  and 79.5%  $\text{N}_2$ ) and pure nitrogen were mixed to generate mixtures with different oxygen concentrations, which were continuously fed through the ozone generator. The flow of nitrogen was kept constant at a value of 1.2 l/min (liters per minute) using a needle valve (NV), and the flow of synthetic air was varied in the range between 0.2 and 1.0 sccm (standard cubic centimeters per minute) by means of a precise mass-flow controller (Tylan FC 260, 10 sccm full range),

in order to obtain different ozone concentrations. The ozone mixture with a flow of about 1 l/min was directly sent to a commercial UV photometric ozone analyzer (Thermal Environmental Instruments Inc., model 49), which has a precision of  $\sim 2$  ppb. Thus, the amount of ozone produced in each mixture was directly determined. Using an attached gas line (see Fig. 1), part of the ozone mixture was pumped with a flow of 168 sccm through the photoacoustic cell. The pressure at the inlets of the PA cell and the UV photometer was kept at the ambient value.

### 3 Wavelength and line-width calibration

Photoacoustic spectra were obtained by scanning the temperature of the QCL from  $-41\text{ }^{\circ}\text{C}$  to  $30.6\text{ }^{\circ}\text{C}$ . Since the photoacoustic signal is proportional to the absorbed light power [12], the obtained PA spectrum scales with the optical absorption spectrum of ozone. However, an appropriate wavelength mapping of the PA spectrum requires accurate knowledge of the dependence of the wavelength on the QCL temperature. For this reason, the PA spectrum of pure  $\text{CO}_2$  gas was measured in the same temperature range employing the same operating conditions, such as the pulse width, pulse period, and current of the QCL. The PA spectrum presented in Fig. 2 shows three absorption peaks, which were assigned to the 9P16, 9P18, and 9P20 lines of the 9P branch of the  $00^0_1 \mu 02^0_0$  rovibrational transition in  $\text{CO}_2$ . Thus the wavelength range corresponding to the  $-41\text{ }^{\circ}\text{C}$  to  $30.6\text{ }^{\circ}\text{C}$  temperature scan could be assigned to the wavenumber range  $1051.8\text{--}1046.3\text{ cm}^{-1}$ .

The line width of the QCL was estimated by convoluting the HITRAN spectrum with an assumed Lorentzian line profile of the QCL. In addition, the HITRAN spectrum was weighted by the measured QCL power. To achieve comparable results the integrals of both the measured PA spectrum and the convoluted HITRAN spectrum were normalized to unity. The best agreement between measured and simulated profiles of the P16 line was obtained by assuming a full width at half maximum (FWHM) of  $0.13\text{ cm}^{-1}$  for the QCL (see Fig. 2). It can be seen, however, that the measured FWHM becomes nar-

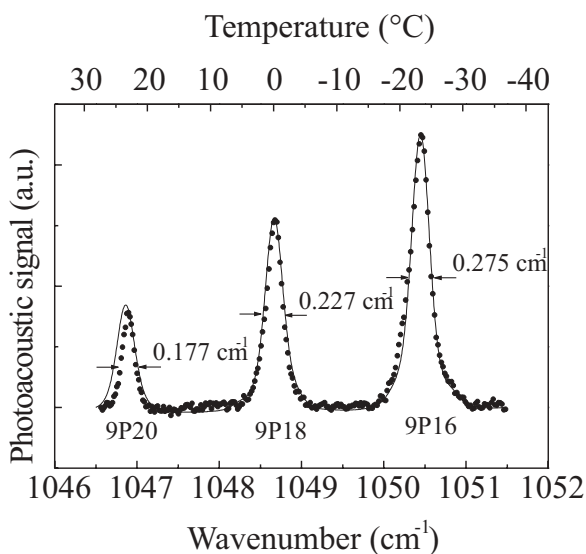


**FIGURE 2** The photoacoustic spectrum of pure  $\text{CO}_2$ . Points: measured PA spectrum; solid line: HITRAN spectrum convoluted with a Lorentzian line shape with  $0.13\text{ cm}^{-1}$  FWHM

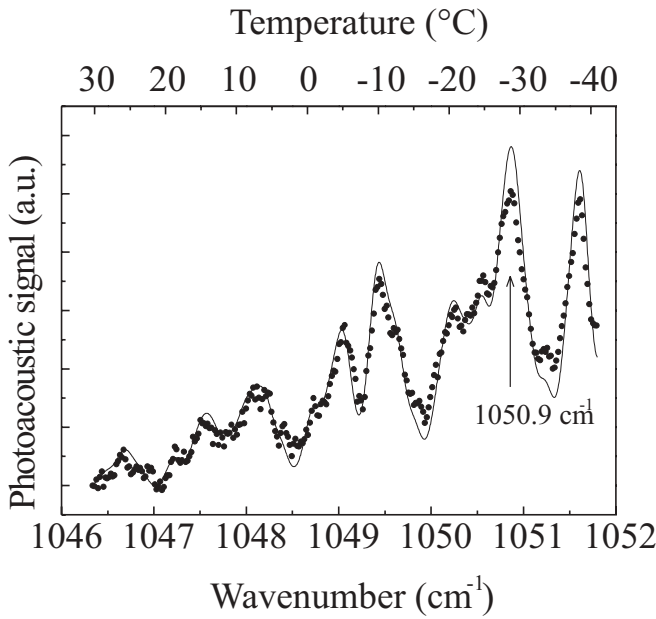


FIGURE 3 PA spectrum of 14 ppmv ozone in an air–nitrogen mixture. Points: measured PA spectrum; solid line: HITRAN spectrum convolved with a Lorentzian line shape of  $0.13 \text{ cm}^{-1}$  FWHM

rower than the convolved one as the temperature increases. This behavior and the FWHM values are in agreement with recently published observations for a similar QCL device [13].

The wavelength calibration and the assumptions on the line profile and line width of the QCL were supported by comparing the convolved HITRAN spectrum of a 14 ppmv ozone–air–nitrogen mixture with the measured PA spectrum as presented in Fig. 3. The overall agreement between the measured and simulated spectra is very good. Several ozone absorption lines can be

recognized in the PA spectrum. The peak at  $1050.9 \text{ cm}^{-1}$  of the  $\nu_3$  vibrational band was selected for the present concentration measurements.

#### 4 Concentration measurements

The photoacoustic signal for different ozone concentrations was measured by keeping the temperature of the QCL at  $-29^\circ\text{C}$  (QCL wavenumber:  $1050.9 \text{ cm}^{-1}$ ). To obtain a higher light power the pulse duration was increased to 50 ns. In order to calibrate the photoacoustic signal the concentration of

ozone in each mixture was determined by the photometric analyzer. Since the commercial ozone generator was unstable for ozone concentrations above 10 ppmv, the present measurements were limited to the 100–4300 ppbv concentration range. The background signal was measured by switching off the ozone generator and flushing the PA cell with pure nitrogen. The acoustic and electronic noise was determined by blocking the laser light while keeping all other devices running. The values of the background and noise signals were typically  $1.7 \mu\text{V}$  and  $0.5 \mu\text{V}$ , respectively.

As expected, a linear dependence of the photoacoustic signal on the ozone concentration was found. The measured PA signals and the fitted straight line are shown in Fig. 4. The smallest measured concentration was 102 ppbv, with a signal-to-background ratio of unity. Thus, the sensitivity realized with the QCL-PA detection system can be estimated as  $\sim 100$  ppbv.

#### 5 Conclusions and outlook

The results presented demonstrate the potential of the photoacoustic technique in combination with a compact quantum cascade laser source in trace-gas detection. Comparing our results with recently published work [13], in which a similar QCL in combination with an optical absorption analysis technique was applied to measure ozone concentrations, an improvement in the ozone-detection sensitivity by a factor of about 200 was achieved by the use of the advanced differential photoacoustic technique. The concentration limit of  $\sim 100$  ppbv reached by direct measurements corresponds to an absorption sensitivity of  $\alpha = 1.24 \times 10^{-6} \text{ cm}^{-1}$ . The corresponding optical density (absorbance) in the 4-cm-long acoustic resonator tube was  $\alpha l = 5 \times 10^{-6}$ . This value is nearly three orders of magnitude better than the corresponding value ( $7 \times 10^{-3}$ ) realized in [13]. Since the photoacoustic signal is proportional to the product of the absorption coefficient and the incident laser power, the performance of a PA detector can be better characterized by the product of the detectable minimum absorption coefficient and the corresponding laser power. In our case this quantity is  $3.7 \times 10^{-9} \text{ W cm}^{-1}$ , in accordance with

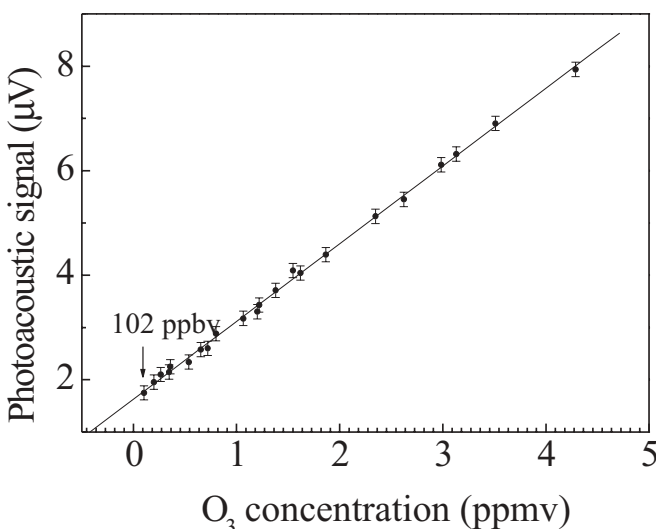


FIGURE 4 Linear dependence of the photoacoustic signal on the ozone concentration at  $1050.9 \text{ cm}^{-1}$

previous investigations with the differential PA detector [14].

Another advantage of the QCL-PA system is its inherent simplicity, in comparison with the setup used in [13], as can be seen in Fig. 1. At present, the most expensive part of the system is the QCL chip. The modulation of the QCL and PA data acquisition and evaluation could be performed by a laptop PC, instead of an expensive lock-in. Consequently, a rugged and versatile QCL-PA instrument can be developed on the basis of the photoacoustic setup. In the analyzed wavenumber range in one of the atmospheric windows, water has a very small absorption cross section, and thus the presented QCL-PA system can be applied to monitor ozone concentrations in ambient air. For this purpose, however, the sensitivity of the system should be increased to about 10 ppbv. This goal can be realized with the QCL-PA system by using a larger-diameter lens and a PA detector with multiple re-

flections specifically optimized for QCL excitation.

**ACKNOWLEDGEMENTS** One of the authors (M.G.S.) thanks CAPES (Brazil) for a scholarship, which made it possible to perform this work during a stay in Heidelberg. Additional financial support by FINEP (Brazil) and Steinbeis GmbH & Co. (Germany) is gratefully acknowledged. We thank K. Mauersberger and T. Roeckmann for fruitful discussions and the opportunity to use the UV photometric ozone analyzer.

#### REFERENCES

- 1 C. Gmachl, A. Straub, R. Colombelli, F. Capasso, D.L. Sivco, A.M. Sergent, A.Y. Cho: IEEE J. Quantum Electron. **QE-38**, 569 (2002)
- 2 B.A. Paldus, T.G. Spence, R.N. Zare, J. Oomens, F.J.M. Harren, D.H. Parker, C. Gmachl, F. Capasso, D.L. Sivco, J.N. Baillargeon, A.L. Hutchinson, A.Y. Cho: Opt. Lett. **24**, 178 (1999)
- 3 C.R. Webster, G.J. Flesch, D.C. Scott, J.E. Swanson, R.D. May, W.S. Woodward, C. Gmachl, F. Capasso, D.L. Sivco, J.N. Baillargeon, A.L. Hutchinson, A.Y. Cho: Appl. Opt. **40**, 321 (2001)
- 4 D. Hofstetter, M. Beck, J. Faist, M. Nägele, M.W. Sigrist: Opt. Lett. **26**, 887 (2001)
- 5 D.D. Nelson, J.H. Shorter, J.B. McManus, M.S. Zahniser: Appl. Phys. B **75**, 343 (2002)
- 6 S. Schilt, L. Thévenaz, E. Courtois, P.A. Robert: Spectrochim. Acta A **58**, 2533 (2002)
- 7 A.A. Kosterev, F.K. Tittel, R. Köhler, C. Gmachl, F. Capasso, D.L. Sivco, A.Y. Cho, S. Wehe, M.G. Allen: Appl. Opt. **41**, 1169 (2002)
- 8 A.A. Kosterev, R.F. Curl, F.K. Tittel, M. Rochat, M. Beck, D. Hofstetter, J. Faist: Appl. Phys. B **75**, 351 (2002)
- 9 T. Beyer, M. Braun, A. Lambrecht: J. Appl. Phys. **93**, 3158 (2003)
- 10 P. Brasseur, J.-F. Müller, X.X. Tie, L. Horowitz: in *Present and Future of Modeling Global Environmental Change: Toward Integrated Modeling*, ed. by T. Matsuno, H. Kida (TERRAPUB, Tokyo 2001) pp. 63–75
- 11 K. Mauersberger, D. Krankowsky, C. Jansson, R. Schinke: in *Advances in Atomic, Molecular, and Optical Physics, Vol. 50*, ed. by B. Benderson, H. Walther (Elsevier, ) 2004)
- 12 A. Miklós, P. Hess, Z. Bozóki: Rev. Sci. Instrum. **72**, 1937 (2001)
- 13 R. Jiménez, M. Taslakov, V. Simeonov, B. Calpini, F. Jeanneret, D. Hofstetter, M. Beck, J. Faist, H. van den Bergh: Appl. Phys. B **78**, 249 (2004)
- 14 A. Schmohl, A. Miklós, P. Hess: Appl. Opt. **40**, 2571 (2001)